ESHG

ARTICLE

Autosomal-dominant adult neuronal ceroid lipofuscinosis caused by duplication in *DNAJC5* initially missed by Sanger and whole-exome sequencing

Ivana Jedličková[1] · Maxime Cadieux-Dion [2,3] · Anna Přistoupilová[1] · Viktor Stránecký[1] · Hana Hartmannová[1] · Kateřina Hodaňová[1] · Veronika Barešová[1] · Helena Hůlková[1,4] · Jakub Sikora [1,4] · Lenka Nosková[1] · Dita Mušálková[1] · Petr Vyleťal[1] · Jana Sovová[1] · Patrick Cossette[2] · Eva Andermann[5] · Frederick Andermann[5] · Stanislav Kmoch[1] · The Adult NCL Gene Discovery Consortium

Abstract

Adult-onset neuronal ceroid lipofuscinoses (ANCL, Kufs disease) are rare hereditary neuropsychiatric disorders characterized by intralysosomal accumulation of ceroid in tissues. The ceroid accumulation primarily affects the brain, leading to neuronal loss and progressive neurodegeneration. Although several causative genes have been identified (*DNAJC5*, *CLN6*, *CTSF*, *GRN*, *CLN1*, *CLN5*, *ATP13A2*), the genetic underpinnings of ANCL in some families remain unknown. Here we report one family with autosomal dominant (AD) Kufs disease caused by a 30 bp in-frame duplication in *DNAJC5*, encoding the cysteine-string protein alpha (CSPα). This variant leads to a duplication of the central core motif of the cysteine-string domain of CSPα and affects palmitoylation-dependent CSPα sorting in cultured neuronal cells similarly to two previously described CSPα variants, p.(Leu115Arg) and p.(Leu116del). Interestingly, the duplication was not detected initially by standard Sanger sequencing due to a preferential PCR amplification of the shorter wild-type allele and allelic dropout of the mutated *DNAJC5* allele. It was also missed by subsequent whole-exome sequencing (WES). Its identification was facilitated by reanalysis of original WES data and modification of the PCR and Sanger sequencing protocols. Independently occurring variants in the genomic sequence of *DNAJC5* encoding the cysteine-string domain of CSPα suggest that this region may be more prone to DNA replication errors and that insertions or duplications within this domain should be considered in unsolved ANCL cases.

These authors contributed equally: Ivana Jedličková, Maxime Cadieux-Dion

✉ Stanislav Kmoch
skmoch@lf1.cuni.cz

1 Research Unit for Rare Diseases, Department of Pediatrics and Adolescent Medicine, First Faculty of Medicine, Charles University, Prague, Czech Republic

2 Centre Hospitalier de L´Universite de Montréal, Montréal, QC, Canada

3 Center for Pediatric Genomic Medicine, Children's Mercy Hospital, Kansas City, MO, USA

4 Institute of Pathology, First Faculty of Medicine and General University Hospital, Charles University, Prague, Czech Republic

5 Montreal Neurological Hospital & Institute, McGill University, Montreal, QC, Canada

Introduction

Adult-onset neuronal ceroid lipofuscinoses (ANCL) constitute a group of rare genetic diseases characterized clinically by the progressive deterioration of mental and motor functions and histopathologically by the intracellular and ultrastructurally distinct accumulation of autofluorescent lipopigment—ceroid—in the brain and other tissues. Age of onset, spectrum of neurological phenotypes, and disease progression can vary even within families. Clinical heterogeneity of ANCLs is in line with diverse inheritance patterns, increasing number of identified causal genes (e.g., *DNAJC5* [1], *CLN6* [2], *CTSF* [3], *GRN* [4], *CLN1* [5], *CLN5* [6], *ATP13A2* [7]), and various types of causative variants and their combinations (NCL Resource—A Gateway for Batten Disease: http://www.ucl.ac.uk/ncl/new nomenclature.shtml).

Diagnosis of ANCLs is challenging from a clinical, histopathologic, as well as diagnostic perspective. Even

with recent technological advances [8, 9], the causative genetic variants(s) in some ANCL families have not been identified. In order to improve genetic diagnosis in these families, we recently established The Adult NCL Gene Discovery Consortium. Within the Consortium we reviewed clinical and histopathological data and classified recruited cases as definite, probable, or possible ANCL or not meeting the diagnostic criteria for ANCL [10]. ANCL cases were then subjected to candidate gene and whole-exome sequencing (WES) [11, 12].

Here we report and characterize a new variant—a **30 base pair in-frame duplication** in *DNAJC5*, that we have identified in one of the investigated ANCL families. The identification of this variant was particularly challenging. It was initially missed by Sanger sequencing of *DNAJC5* and WES, to be identified later by reanalysis of original WES data that were shared within the Consortium. Our work thus also provides a cautionary tale about the challenges in identification of even relatively short insertions and duplications by standard genetic methods.

Materials and methods

Subjects

The study protocol was approved by the local Institutional Review Boards and signed informed consent was obtained from all subjects.

The Canadian family was ascertained at the Montreal Neurological Institute, McGill University, Canada based on clinical observation of three affected individuals: a mother and two sons. The mother was diagnosed with Kufs disease at the age of 42 and died at the age of 56 (no clinical details are available). The affected sons presented with seizures, memory loss, and disability (wheelchair bound) at the age of 31 and 34. No biopsy material for pathological evaluation was available at the time of investigation to examine for the presence of typical lipopigment in tissues of affected individuals.

DNA sequencing and variant analysis

Genomic DNA of the two brothers was extracted from whole blood samples by a standard protocol. Coding regions of *DNAJC5* (NG_029805.2) were amplified by PCR from genomic DNA of the two brothers and sequenced by direct Sanger sequencing using the version 3.1 Dye Terminator cycle sequencing kit (ThermoFisher Scientific) with electrophoresis on an ABI 3500XL Avant Genetic Analyzer (ThermoFisher Scientific). Data were analyzed using Sequencing Analysis software (ThermoFisher Scientific).

Exome sequencing

Exome sequencing was performed using genomic DNA from the two affected brothers (Fig. 1). For DNA enrichment, the Sure Select Human All Exon V4 capture kit (Agilent Technologies, Santa Clara, CA) was used according to the manufacturer's protocol. DNA sequencing was performed on the captured barcoded DNA library via an Illumina HiSeq 2000 system as a pair end library with the read length of 100 bp. The resulting FASTQ files were aligned to the human reference genome (hg19) via BWA-MEM [13]. After genome alignment, conversion of SAM format to BAM and duplicate removal were performed using Picard Tools (1.129). The Genome Analysis Toolkit, GATK (3.2.2) [14–16] was used for local realignment around indels, base recalibration, variant recalibration, and variant calling (HaplotypeCaller). Variant annotation was performed with SnpEff 3.6 [17] and GEMINI 0.18.2 [18].

In silico analysis of the cysteine-string domain

Hydrophobicity and palmitoylation potential of the wild-type (wt) cysteine-string domain (CSD) and the CSD carrying the *DNAJC5* variant were analyzed with a Kyte–Doolittle algorithm and CSS-Palm 2.0, respectively, as described previously [1].

CSPα-expression vectors

DNAJC5/CSPα cDNA was amplified by RT-PCR from the affected individuals' leukocytes with specific primers. Resulting PCR products were first cloned into PCR2.1 TOPO TA-cloning vector (Invitrogen) and, after sequencing verification, the cDNA region containing the 30 bp duplication was subcloned into a pEGFP-C1/DNAJC5 wt vector using BstXI and BsmBI restriction sites. The pEGFP-C1/DNAJC5_wt, pEGFP-C1/DNAJC5_Leu115Arg, and pEGFP-C1/DNAJC5_Leu116del vectors were generated as described previously [1].

Transient expression of EGFP–CSPα

cDNA constructs were transfected into CAD5 cells derived from Cath. -a-differentiated (CAD) cells (provided by Sukhvir Mahal, The Scripps Research Institute, Jupiter, FL, USA). Four to seven days before transfection, 1×10^4 cells/cm^2 were seeded with Opti-MEM medium (Opti-MEM; Invitrogen) containing 10% FBS (HyClone, Logan, UT), 90 units penicillin, streptomycin/ml. Cells were transfected by either 0.8 or 4 μg of plasmid constructs with Lipofectamine 2000 (Invitrogen) in serum and antibiotics free Opti-MEM medium according to the
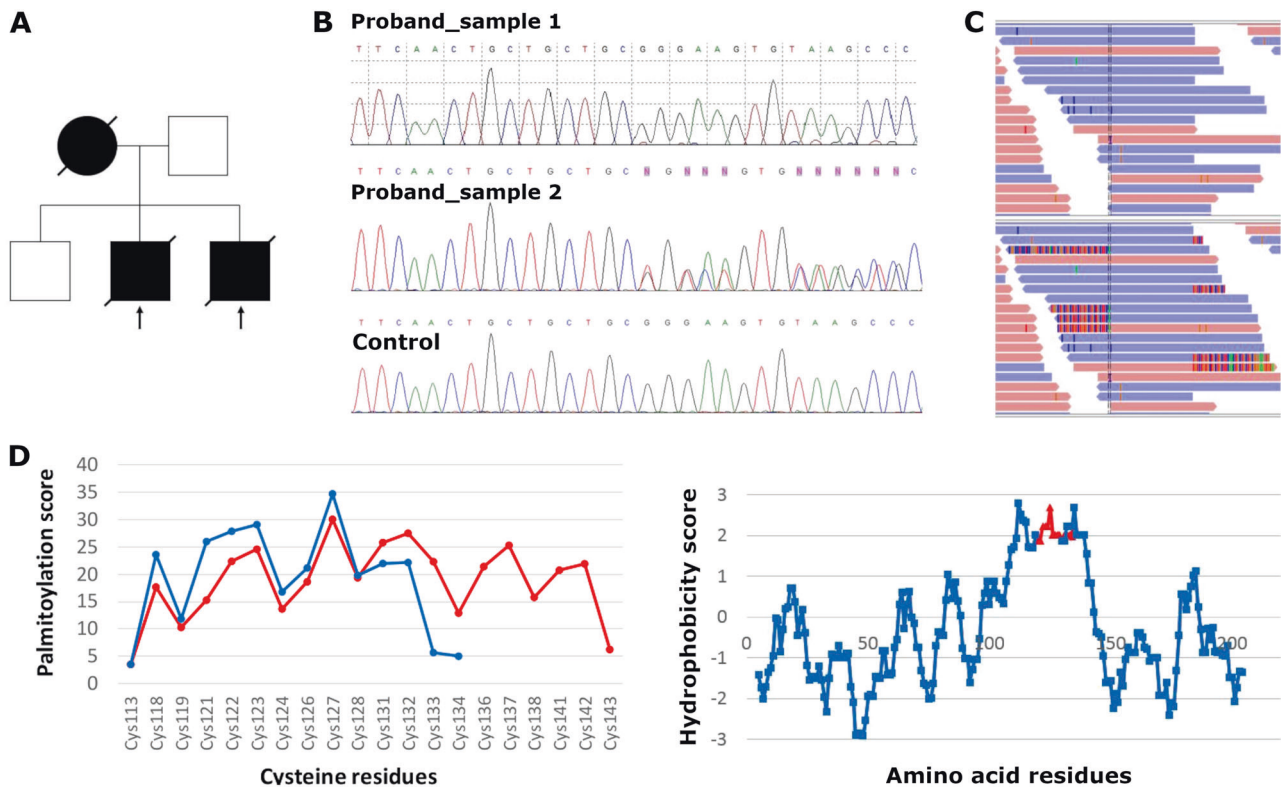
Fig. 1 Sanger sequencing and reads alignment of the *DNAJC5* bearing the 30 bp duplication. a Pedigree of the Canadian family suggesting an autosomal dominant inheritance. **b** Chromatograms of *DNAJC5* genomic DNA sequences showing normal *DNAJC5* sequence in the proband using original protocol (Proband_sample 1) and heterozygous duplication in the same DNA sample upon modified PCR protocol (Proband_sample 2). Lower panel shows chromatogram from control DNA. **c** The 30 bp duplication in *DNAJC5* in the

Integrative Genomics Viewer (IGV2.3) before (upper panel) and after a visualization of soft-clipped bases (lower panel). **d** In silico analysis of the cysteine-string domain showing that compared with the wild-type sequence (blue line), the duplication (red line) alters palmitoylation potential (left panel) and hydrophobicity profile (right panel), critical parameters of post-translational modification, and intracellular localization of CSPα.

manufacturer's protocol. Transfection experiments were performed in more than three replicates.

Immunofluorescence analysis

Cells were fixed 24 h after transfection with chilled methanol for 10 min, washed, blocked with 5% bovine serum albumin (BSA), and incubated for 1 h at 37 °C with antiprotein disulfide isomerase mouse monoclonal IgG1 (Stressgen, San Diego, CA) for endoplasmic reticulum (ER) localization, anti-GS28 mouse IgG1 (Stressgen, San Diego, CA) for Golgi localization, and anti-GFP rabbit polyclonal IgG (Abcam) for EGFP-CSPα detection. For fluorescence detection, corresponding species-specific secondary antibodies Alexa Fluor 488 and Alexa Fluor 555 (Molecular Probes, Invitrogen, Paisley, UK) were used. Prepared slides were mounted in ProLong® Gold Antifade with 4′,6-diamidino-2-phenylindole staining nuclei (Life Technologies, Forster City, USA) fluorescence mounting medium and analyzed by confocal microscopy.

Image acquisition and analysis

Prepared slides were analyzed by confocal microscopy. XYZ images were sampled according to Nyquist criterion using a LeicaSP8X laser scanning confocal microscope, HC PL APO objective (63×, N.A. 1.40), 405, 488, and 543 laser lines. Images were restored using a classic maximum likelihood restoration algorithm in the Huygens Professional Software (SVI, Hilversum, The Netherlands) [19]. The colocalization maps employing single pixel overlap coefficient values ranging from 0 to 1 were created in the Huygens Professional Software [20]. The resulting overlap coefficient values are presented as the pseudo color denoted in the corresponding lookup tables.

Immunoblot analysis

Transfected CAD5 cells were harvested in PBS, centrifuged at $610 \times g$ for 5 min, resuspended in 50 mM Tris pH 6.8, 50 mM DTT, 2% sodium dodecyl sulfate (SDS), and Complete Protease Inhibitor Cocktail (Roche) or PBS with

Triton X-100, 0.1 or 0.5% and Complete Protease Inhibitor Cocktail (Roche), homogenized by sonication using the Covaris S2 Ultrasonicator, followed by denaturation at 100 °C for 10 min. The protein content in the supernatant was determined using an infrared spectrometer Direct Detect infrared (Millipore) according to the manufacturer's protocol. Protein lysates equivalent to 15 or 20 µg of protein were incubated with and without 6 M hydroxylamine for CSPα depalmitoylation for 24 h at room temperature and reduced at 100 °C for 5 min in sample buffer with or without 1% beta-mercaptoethanol (βME) before SDS-PAGE electrophoresis. After protein transfer to the polyvinylidene fluoride membrane, membranes were blocked by 5% milk and 0.1% Tween 20 in PBS over night at 4 °C. CSPα or CSPα-EGFP protein was visualized by incubation with rabbit CSP antibody (Stressgen) at 1:5000 in 0.1% BSA and 0.1% Tween 20 in PBS for 60 min or rabbit green fluorescent protein (GFP) antibody (Abcam) at 1:3000 in 0.1% BSA and 0.1% Tween 20 in PBS for 60 min, followed by incubation with goat antirabbit HRP (Pierce) at 1:10,000 in 0.1% Tween 20 in PBS for 60 min and detection by Clarity Western ECL Substrate (Bio-Rad).

Results

Identification of 30 base pair duplication in *DNAJC5* by a combination of exome sequencing and sanger sequencing

To identify the genetic lesion in affected family members we initially Sanger sequenced and excluded *DNAJC5*, the prevalent gene for autosomal dominant ANCL (AD-ANCL) (Fig. 1b). Next we sequenced all coding exons and 5′ and 3′ untranslated regions of their corresponding mRNAs (UTRs) (Sure Select Human All Exon V4 capture kit, Illumina HiSeq 2000) in both affected brothers. Considering an autosomal dominant model of inheritance, we searched for variants that had standard read count threshold ≥10, were present in the heterozygous state in both affected individuals and had a minor allele frequency <0.5% in The Exome Aggregation Consortium database [21]. These parameters did not yield any functionally relevant candidate variant. Lowering the standard read count threshold to ≥5, we found a 30 bp in-frame duplication in *DNAJC5*. This variant was however not seen in the IGV tool, which allows visualization of sequence alignments. Essential for the variant detection was a visualization of so called soft-clipped bases, which are reads not matching with the reference sequence in their whole length. Using the visualization of soft-clipped bases we revealed the 30 bp in-frame duplication: chr20:g.62562252_62562281dup (hg19); NM_025219.2:c.370_399dup (p.(Cys124_Cys133dup)), in

exon 4 of *DNAJC5*. (Fig. 1c). We modified our original PCR protocol and confirmed the presence of the duplication using standard Sanger sequencing (Fig. 1a, upper panels). The variant was submitted to ClinVar database under the accession code VCV000689476 and to the Mutation and Patient Database for Human NCL genes [22].

In silico analysis of the novel CSPα c.370_399dup (p.(Cys124_Cys133dup)) variant

The duplication encodes for a duplication of the central core motif of the CSD of CSPα. NM_025219.2:c.370_399dup (p.(Cys124_Cys133dup)). The CSD is implicated in palmitoylation and membrane trafficking of CSPα. In silico analysis suggested that the duplication increases hydrophobicity (Fig. 1d, right panel) of the CSD and that the presence of the additional seven cysteine residues changes the palmitoylation potential (Fig. 1d, left panel). Changes in these parameters can make the protein carrying the p.(Cys124_Cys133dup) variant prone to aggregation [23].

The functional effect of the GFP-tagged CSPα p.(Cys124_Cys133dup) variant in neuronal CAD5 cell model

To assess the effect of the identified duplication on CSPα expression and intracellular localization we transiently expressed N-terminal GFP tagged CSPα with the identified duplication p.(Cys124_Cys133dup), wt CSPα (GFP_CSPα_wt) and GFP_CSPα with previously identified variants NM_025219.2:c.344T>G (p.(Leu115Arg)) and NM_025219.2:c.343_345del (p.(Leu116del)), both variants located in exon 4 of *DNAJC5* (the exon numbering starts with exon 1 to exon 5), shortly p.(Leu115Arg) and p.(Leu116del), in CAD5 cells. Immunofluorescence analysis and colocalization studies showed that the GFP_CSPα_wt and the endogenous CSPα are localized dominantly along the plasma membrane in finely granular cytoplasmic structures. All three GFP_CSPα proteins with the variants p.(Cys124_Cys133dup), p.(Leu115Arg), and p.(Leu116del) had reduced expression on the plasma membrane. They are present mostly in cytoplasm, either in a diffuse form or as a coarsely granular inclusions that colocalize to a certain extent with markers of ER and Golgi apparatus (Fig. 2, Supplementary Fig. 1).

Immunoblot analysis of GFP-CSPα transiently produced in CAD5 cells

To assess the effect of the identified duplication we performed western blot analysis of transiently transfected CAD5 cell lysates before and after chemical depalmitoylation performed under different denaturing conditions
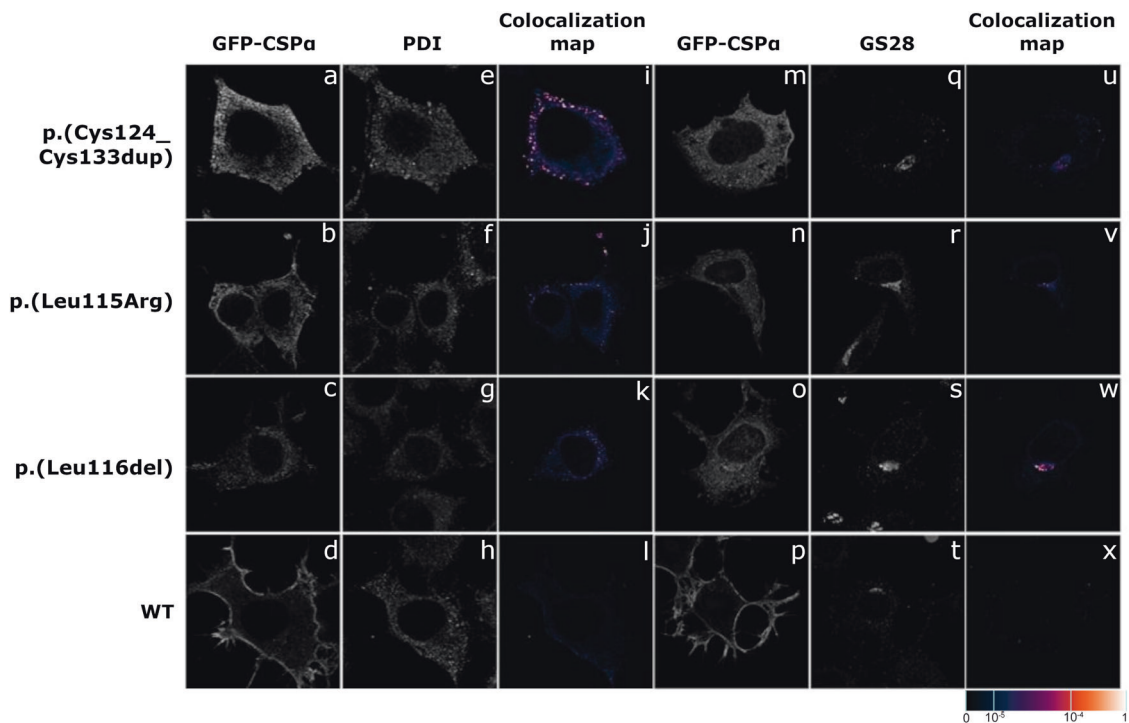
Fig. 2 Immunofluorescence analysis of transiently expressed GFP-tagged CSPα wt and variant proteins in CAD5 cells. All three variant proteins (**a–c**, **m–o**) are present in a finely or coarsely granular structures. Co-staining with (**e–g**) protein disulfide isomerase (PDI), a marker of endoplasmic reticulum (ER), and (**q–s**) Golgi SNAP receptor complex member 1 (GS28) demonstrates abnormal presence of mutated proteins in ER (**i–k**) and Golgi (**u–w**). Wild-type protein (**d**, **h**, **l**, **p**, **t**, **x**) is present exclusively on plasma membrane. The degree of colocalization of GFP_CSPα with selected markers is demonstrated by the fluorescent signal overlap coefficient values ranging from 0 to 1. The resulting overlap coefficient values are presented as the pseudo color whose scale is shown in corresponding lookup table.

(Fig. 3). We found that the GFP_CSPα protein carrying the Cys124_Cys133dup is present exclusively in non-palmitoylated form, whereas GFP_CSPα_Leu115Arg and GFP_CSPα_Leu116del proteins can present in both, the nonpalmitoylated or palmitoylated CSPα with the former more abundant. All three GFP_CSPα_Leu115Arg, GFP_CSPα_Leu116del, and GFP_CSPα_Cys124_Cys133dup proteins formed high molecular weight aggregates that were resistant to SDS and reducing agents (DTT, βME). The aggregates became soluble by these procedures only upon initial chemical depalmitoylation by hydroxylamine (Fig. 3).

Discussion

In this work we identified a 30 bp duplication in *DNAJC5* encoding CSPα in one family ascertained by The Adult NCL Gene Discovery Consortium. The variant leads to a duplication of the central core motif of the CSD and affects palmitoylation-dependent CSPα sorting in cultured neuronal cells similar to two other previously described single nucleotide CSPα variants p.Leu115Arg and p.Leu116del. CSPα acts as a co-chaperone in the formation of presynaptic SNARE complexes (soluble N-ethylmaleimide-sensitive

factor attachment protein receptors) [24]. The SNAREs are essential for docking of synaptic vesicles, their fusion and recycling. There is accumulating evidence that disruption of the SNARE machinery leads to neurodegeneration [25].

This family remained genetically undefined for decades. Initially, the variant could not be detected by standard Sanger sequencing of *DNAJC5* probably due to a preferential PCR amplification of the shorter wt allele and allelic dropout of the mutated *DNAJC5* allele. It was also missed by a subsequent analysis of WES. Its identification was facilitated by reanalysis of the original WES data shared within the Consortium and modification of the PCR and Sanger sequencing protocols.

Independently occurring variants in the genomic sequence of *DNAJC5* encoding the CSD of CSPα [1] suggest that this region may be more prone to DNA replication errors and that insertions or duplications within this domain should be considered in not yet solved ANCL cases.

Our work demonstrates the limitations of Sanger sequencing and WES in detection of even relatively small insertions and duplications and shows that analysis of next generation sequence data still requires an individualized approach and unique interpretations of the data. Continued reanalysis of the data with a team of experienced scientists
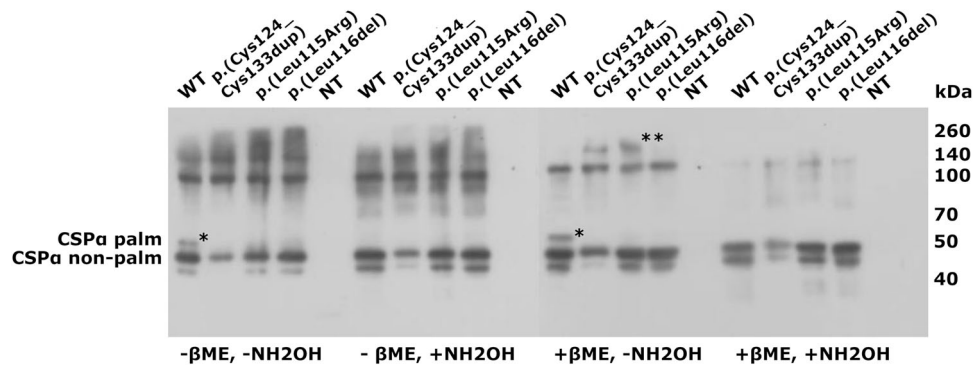
Fig. 3 Immunoblot analysis of transiently expressed GFP-tagged CSPα proteins in CAD5 cells. Immunodetection using the CSP antibody reveals that the GFP_CSPα_p.(Cys124_Cys133dup) protein is present exclusively in nonpalmitoylated form (CSPα nonpalm; the asterisk (*) refers to the palmitoylated form—CSPα palm). All three GFP_CSPα proteins with the variants p.(Leu115Arg), p.(Leu116del), p.(Cys124_Cys133dup) form high molecular weight aggregates (**) resistant to sodium dodecyl sulfate (SDS) and reducing agents (DTT, βME). The aggregates are soluble only upon initial chemical depalmitoylation by hydroxylamine (NH2OH).

may identify previously missed variants. Approximately 75% of patients with neurodegeneration subjected to WES remain without a genetic diagnosis [26]. It is unclear how many similar variants will be identified by continued reanalysis, as demonstrated in this paper.

Data availability

The authors state that anonymized data will be shared by request from any qualified investigator.

Compliance with ethical standards

Conflict of interest The authors declare that they have no conflict of interest.

Publisher's note Springer Nature remains neutral with regard to jurisdictional claims in published maps and institutional affiliations.

References

1. Noskova L, Stranecky V, Hartmannova H, Pristoupilova A, Baresova V, Ivanek R, et al. Mutations in DNAJC5, encoding cysteine-string protein alpha, cause autosomal-dominant adult-onset neuronal ceroid lipofuscinosis. Am J Hum Genet. 2011;89:241–52.

2. Arsov T, Smith KR, Damiano J, Franceschetti S, Canafoglia L, Bromhead CJ, et al. Kufs disease, the major adult form of neuronal ceroid lipofuscinosis, caused by mutations in CLN6. Am J Hum Genet. 2011;88:566–73.

3. Smith KR, Dahl HH, Canafoglia L, Andermann E, Damiano J, Morbin M, et al. Cathepsin F mutations cause Type B Kufs disease, an adult-onset neuronal ceroid lipofuscinosis. Hum Mol Genet. 2013;22:1417–23.

4. Smith KR, Damiano J, Franceschetti S, Carpenter S, Canafoglia L, Morbin M, et al. Strikingly different clinicopathological phenotypes determined by progranulin-mutation dosage. Am J Hum Genet. 2012;90:1102–7.

5. van Diggelen OP, Thobois S, Tilikete C, Zabot MT, Keulemans JL, van Bunderen PA, et al. Adult neuronal ceroid lipofuscinosis with palmitoyl-protein thioesterase deficiency: first adult-onset patients of a childhood disease. Ann Neurol. 2001;50:269–72.

6. Xin W, Mullen TE, Kiely R, Min J, Feng X, Cao Y, et al. CLN5 mutations are frequent in juvenile and late-onset non-Finnish patients with NCL. Neurology. 2010;74:565–71.

7. Bras J, Verloes A, Schneider SA, Mole SE, Guerreiro RJ. Mutation of the parkinsonism gene ATP13A2 causes neuronal ceroid-lipofuscinosis. Hum Mol Genet. 2012;21:2646–50.

8. Cotman SL, Karaa A, Staropoli JF, Sims KB. Neuronal ceroid lipofuscinosis: impact of recent genetic advances and expansion of the clinicopathologic spectrum. Curr Neurol Neurosci Rep. 2013;13:366.

9. Kmoch S, Stranecky V, Emes RD, Mitchison HM. Bioinformatic perspectives in the neuronal ceroid lipofuscinoses. Biochim Biophys Acta. 2013;1832:1831–41.

10. Berkovic SF, Staropoli JF, Carpenter S, Oliver KL, Kmoch S, Anderson GW, et al. Diagnosis and misdiagnosis of adult neuronal ceroid lipofuscinosis (Kufs disease). Neurology. 2016;87:579–84.

11. Ehling R, Noskova L, Stranecky V, Hartmannova H, Pristoupilova A, Hodanova K, et al. Cerebellar dysfunction in a family harboring the PSEN1 mutation co-segregating with a cathepsin D variant p.A58V. J Neurol Sci. 2013;326:75–82.

12. van den Ameele J, Jedlickova I, Pristoupilova A, Sieben A, Van Mossevelde S, Ceuterick-de Groote C, et al. Teenage-onset progressive myoclonic epilepsy due to a familial C9orf72 repeat expansion. Neurology. 2018;90:e658–e663.

13. Li H. Aligning sequence reads, clone sequences and assembly contigs with BWA-MEM. Bioinformatics. 2013;00:1–2.

14. McKenna A, Hanna M, Banks E, Sivachenko A, Cibulskis K, Kernytsky A, et al. The Genome Analysis Toolkit: a MapReduce framework for analyzing next-generation DNA sequencing data. Genome Res. 2010;20:1297–303.

15. DePristo MA, Banks E, Poplin R, Garimella KV, Maguire JR, Hartl C, et al. A framework for variation discovery and genotyping using next-generation DNA sequencing data. Nat Genet. 2011;43:491–8.

16. Van der Auwera GA, Carneiro MO, Hartl C, Poplin R, Del Angel G, Levy-Moonshine A, et al. From FastQ data to high confidence variant calls: the Genome Analysis Toolkit best practices pipeline. Curr Protoc Bioinform. 2013;43:11 10 1–33.

17. Cingolani P, Platts A, Wang le L, Coon M, Nguyen T, Wang L, et al. A program for annotating and predicting the effects of single nucleotide polymorphisms, SnpEff: SNPs in the genome of Drosophila melanogaster strain w1118; iso-2; iso-3. Fly. 2012;6:80–92.

18. Paila U, Chapman BA, Kirchner R, Quinlan AR. GEMINI: integrative exploration of genetic variation and genome annotations. PLoS Comput Biol. 2013;9:e1003153.

19. Landmann L. Deconvolution improves colocalization analysis of multiple fluorochromes in 3D confocal data sets more than filtering techniques. J Microsc. 2002;208(Pt 2):134–47.

20. Manders EMM, Verbeek FJ, Aten JA. Measurement of colocalization of objects in dual-color confocal images. J Microsc. 1993;169:375–82.

21. Lek M, Karczewski KJ, Minikel EV, Samocha KE, Banks E, Fennell T, et al. Analysis of protein-coding genetic variation in 60,706 humans. Nature. 2016;536:285–91.

22. Mole SE, Gardener E. Mutation and patient database for human NCL genes. 2019. https://www.ucl.ac.uk/ncl-disease/mutation-and-patient-database/mutation-and-patient-datasheets-human-ncl-genes. Accessed 22 Oct 2019.

23. Diez-Ardanuy C, Greaves J, Munro KR, Tomkinson NC, Chamberlain LH. A cluster of palmitoylated cysteines are essential for aggregation of cysteine-string protein mutants that cause neuronal ceroid lipofuscinosis. Sci Rep. 2017;7:10.

24. Burgoyne RD, Morgan A. Cysteine string protein (CSP) and its role in preventing neurodegeneration. Semin Cell Dev Biol. 2015;40:153–9.

25. Gorenberg EL, Chandra SS. The role of co-chaperones in synaptic proteostasis and neurodegenerative disease. Front Neurosci. 2017;11:248.

26. Fogel BL. Genetic and genomic testing for neurologic disease in clinical practice. Handb Clin Neurol. 2018;147:11–22.